

Investigating the Corruption Robustness of Image Classifiers with Random p -norm Corruptions

Georg Siedel^{1,2}, Weijia Shao¹, Silvia Vock¹, Andrey Morozov²

¹*Federal Institute for Occupational Safety and Health (BAuA), Dresden, Germany*

²*University of Stuttgart, Germany*

{siedel.georg, shao.weijia, vock.silvia}@baua.bund.de, andrey.morozov@ias.uni-stuttgart.de

Keywords: image classification, corruption robustness, p -norm

Abstract: Robustness is a fundamental property of machine learning classifiers required to achieve safety and reliability. In the field of adversarial robustness of image classifiers, robustness is commonly defined as the stability of a model to all input changes within a p -norm distance. However, in the field of random corruption robustness, variations observed in the real-world are used, while p -norm corruptions are rarely considered. This study investigates the use of random p -norm corruptions to augment the training and test data of image classifiers. We assess the model robustness against imperceptible random p -norm corruptions and propose a novel robustness metric. We empirically investigate whether robustness transfers across different p -norms and derive conclusions on which p -norm corruptions a model should be trained and evaluated. We find that training data augmentation with a combination of p -norm corruptions improves corruption robustness significantly, even on top of state-of-the-art data augmentation schemes.

1 INTRODUCTION

State-of-the-art computer vision models achieve human-level performance in various tasks, such as image classification (Krizhevsky et al., 2017). This makes them potential candidates for sophisticated vision tasks. However, they tend to be easily fooled by small changes in their input data, which limits their overall dependability to perform in safety-critical applications (Carlini and Wagner, 2017). For classification models, robustness against small data changes is therefore considered a fundamental pillar of AI dependability and has attracted considerable research interest in recent years.

The most attention within the robustness research landscape is on the adversarial robustness domain (Drenkow et al., 2021). An adversarial attack aims to find worst-case counterexamples for robustness. However, vision models are not only vulnerable to small worst-case data manipulations in the input data but also to randomly corrupted input data (Dodge and Karam, 2017). Accordingly, the corruption robustness¹ domain aims at models that perform similarly well on data corrupted with random noise. Adversarial robustness and corruption robustness need

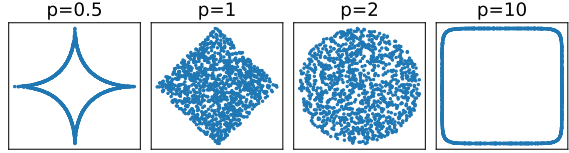


Figure 1: Samples drawn uniformly in 2D from a $L_{0.5}$ and a L_{10} norm sphere (left and right) and a L_1 and a L_2 norm ball (middle).

to be clearly distinguished: Existing research suggests that these two types of robustness target different model properties and applications (Wang et al., 2021). Also, adversarial robustness and corruption robustness do not necessarily transfer to each other, and adversarial robustness is much harder to achieve in high-dimensional input space (Fawzi et al., 2018a; Ford et al., 2019).

1.1 Motivation

The adversarial robustness domain provides the clearest definition of robustness based on a maximum manipulation distance in the p -norm space (see Section 2.1) (Drenkow et al., 2021). Accordingly, there exists a set of p -norms and maximum distances ϵ for each norm that are common for the robustness evaluation on popular image classification benchmarks, e.g. L_∞

¹Also called statistical robustness

with $\epsilon = 8/255$ and L_2 with $\epsilon = 0.5$ on the benchmark datasets CIFAR and SVHN (Croce and Hein, 2020; Yang et al., 2020).

In contrast, corruption robustness is commonly assessed by testing data corruptions originating from camera, hardware, or environment (Hendrycks and Dietterich, 2019). Such data corruptions can occur in real-world applications². Investigating robustness using p -norm distances is rarely employed in the corruption robustness domain. We present three arguments to motivate our investigation into this area.

First of all, the adversarial robustness targets the significant performance degradation caused by p -norm manipulations, which are small or, even worse, imperceptible (Carlini and Wagner, 2017; Szegedy et al., 2013; Zhang et al., 2019). From our point of view, a classifier should generalize in line with human perception, regardless of whether the manipulations are adversarial or random. Therefore, we want to investigate if the same holds for random p -norm corruptions.

Secondly, related works have shown that increasing the range of training data augmentations can improve the performance of classifiers (Mintun et al., 2021; Müller and Hutter, 2021). Therefore, we expect that combining different p -norm corruptions at training time leads to effective robustness improvements.

Furthermore, studies have shown the difficulty of predicting transferability among different types of corruption (Hendrycks and Dietterich, 2019; Ford et al., 2019). Considering the large differences between the volumes covered by different p -norm balls in high dimensional space (see Table 6 in the appendix), we conjecture the same for different p -norm corruptions, which should be observable in the empirical evaluation.

1.2 Contributions

This paper investigates image classifiers trained and tested on random p -norm corruptions.³ The main contributions can be summarized as follows:

- We propose to test classifiers on random quasi-imperceptible corruptions from different p -norms and demonstrate a performance degradation. We propose to measure this minimum requirement for corruption robustness with a corresponding robustness metric.
- We present an empirically effective training data augmentation strategy based on combinations of

²Hence, we call them "real-world corruptions", even though they are generally artificially created

³Code available: <https://github.com/Georgsiedel/Lp-norm-corruption-robustness>

p -norm corruptions that improve robustness with little negative impact on accuracy.

- We evaluate how robustness obtained from training on p -norm corruptions transfers to other p -norm corruptions and to real-world corruptions. We discuss the transfer of p -norm corruption robustness from a test coverage perspective.

2 PRELIMINARIES

2.1 Robustness definition

A classifier g is locally robust at a data point x within a distance $\epsilon > 0$, if $g(x) = g(x')$ holds for all perturbed points x' that satisfy

$$\text{dist}(x, x') \leq \epsilon \quad (1)$$

with x' close to x according to a predefined distance measure (Carlini and Wagner, 2017).

In the adversarial attack domain (Carlini and Wagner, 2017), this distance in \mathbb{R}^d is commonly induced by a p -norm (Weng et al., 2018; Yang et al., 2020), for $0 \leq p \leq \infty$ ⁴:

$$\|x - x'\|_p = (\sum_{i=1}^d |x_i - x'_i|^p)^{1/p}. \quad (2)$$

2.2 Sampling algorithm

In order to experiment with random corruptions uniformly distributed within a p -norm ball or sphere, an algorithm that scales to high-dimensional space is required for all norms $0 < p < \infty$ ⁵. We use the approach in (Calafiori et al., 1998), the detailed description of which is available in the appendix.

Figure 1 visualises samples for different p -norm unit balls in \mathbb{R}^2 using the proposed algorithm, demonstrating its ability to sample uniformly inside the ball and on the sphere.

3 RELATED WORK

p -norm Distances in the Robustness Context As described in Section 2.1, p -norm distances are used to define adversarial robustness. Moreover, p -norm distances have been used to measure certain properties of image data related to robustness. One such property

⁴Here, we abuse the term "norm distance" by also using $0 \leq p < 1$, which are no norms by mathematical definition.

⁵ $p = 0$ (set a ratio ϵ of dimensions to 0 or 1) and $p = \infty$ (add uniform random value from $[\epsilon, -\epsilon]$ to every dimension) are trivial from a sampling perspective.

is the threshold at which an image manipulation is imperceptible, which is a reference point in the field of adversarial robustness (Szegedy et al., 2013). L_∞ manipulations with $\epsilon = 8/255$ have been used in conjunction with the imperceptibility threshold (Zhang et al., 2019; Madry et al., 2017). However, the justification of an exact imperceptibility threshold is difficult (Zhang et al., 2019). Researchers have therefore called for further research into "distance metrics closer to human perception" (Huang et al., 2020). There exist similarity measures for images that are more aligned with human perception than p -norm distances (Wang et al., 2004). To the best of our knowledge, these measures have not yet been used as distance measures for the robustness evaluation of perception models.

Another property of image data measured using p -norm distances in the context of robustness is the class separation of a dataset. The average class separation is used by (Fawzi et al., 2018b) in order to obtain a comparable baseline distance for robustness testing. Similarly, (Yang et al., 2020) measure the minimum class separation on typical image classification benchmarks using L_∞ -distances. The authors conclude the existence of a perfectly robust classifier with respect to this distance. Based on this idea, (Siedel et al., 2022) investigate robustness on random L_∞ -corruptions with minimum class separation distance in order to obtain a more interpretable robustness metric.

(Wang et al., 2021) test and train image classifiers on data corrupted by few random L_∞ corruptions. Overall, little research has been directed at using random corruptions based on p -norm distances to evaluate robustness.

Real-world Data Corruption for Testing In comparison, plenty of research uses real-world data corruption to evaluate corruption robustness, like the popular corruption benchmark by (Hendrycks and Dietterich, 2019) and extensions thereof like in (Mintun et al., 2021).

Real-world Data Corruption for Training Real-world data corruptions are also used as training data augmentations alongside geometric transformations in order to obtain better generalizing or more robust classifiers (Shorten and Khoshgoftaar, 2019). Some training data augmentations target only accuracy but not robustness (Cubuk et al., 2020; Müller and Hutter, 2021). A few approaches use only geometric transformations, such as cuts, translations and rotations, to improve overall robustness (Yun et al., 2019; Hendrycks et al., 2019). Some approaches make use of random noise, such as Gaussian and Impulse noise, to improve robustness (Lopes et al., 2019;

Dai and Berleant, 2021).

Even though accuracy and robustness have long been considered as an inherent trade-off (Tsipras et al., 2019; Zhang et al., 2019). Several described data augmentation methods manage to increase corruption robustness along with accuracy (Hendrycks et al., 2019; Lopes et al., 2019). Some data augmentation methods even leverage random corruptions to implicitly or explicitly improve or give guarantees for adversarial robustness (Cohen et al., 2019; Weng et al., 2019; Lecuyer et al., 2019; Yun et al., 2019).

Classic Noise and p -norm Corruptions Some perturbation techniques used in signal processing are closely related to p -norm corruptions. Gaussian noise shares similarities with L_2 -norm corruptions (Cohen et al., 2019). Impulse Noise or Salt-and-Pepper Noise are similar to this paper's notion of L_0 -norm corruptions. Applying brightness or darkness to an image is a non-random L_∞ corruption that applies the same change to every pixel. This similarity further motivates our investigation of the behaviour of various p -norm corruptions.

Robustness Transferability Robustness is typically specific to the type of corruption or attack the model was trained for. Only to a limited extent are adversarial or corruption robustness transferable between each other (Fawzi et al., 2018a; Fawzi et al., 2018b; Rusak et al., 2020), across different p -norm attacks and attack strengths (Carlini et al., 2019), or across real-world corruption types (Hendrycks and Dietterich, 2019; Ford et al., 2019). This finding motivates our investigation into whether random p -norm corruption robustness transfers to other p -norm corruptions and real-world corruptions.

Wide Training Data Augmentation Recent efforts suggest that choosing randomly from a wide range of augmentations can be more effective compared to more sophisticated augmentation strategies (Mintun et al., 2021; Müller and Hutter, 2021). This finding encourages our investigation of combining training time p -norm corruptions that effectively improve corruption robustness.

4 EXPERIMENTAL SETUP

4.1 Robustness Metrics

Additionally to the standard test error E_{clean} , we use 4 metrics to assess the corruption robustness of all our trained models. For all reported metrics, low numbers indicate a better performance.

To cover well-known real-world corruptions, we compute the **mCE (mean Corruption Error)** metric

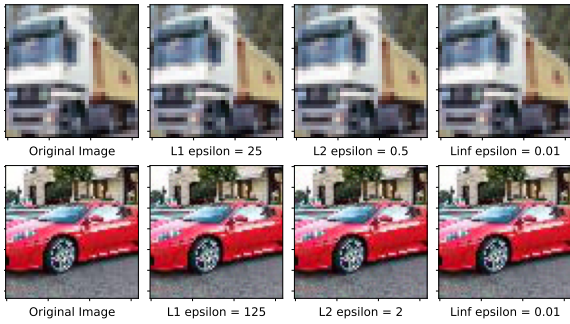


Figure 2: Examples from the chosen set of imperceptible corruptions on CIFAR (above) and TinyImageNet (below)

using the benchmark by (Hendrycks and Dietterich, 2019). We use a 100% error rate as a baseline, so that **mCE** corresponds to the average error rates \mathbf{E} across 19 different corruptions \mathbf{c} and 5 corruption severities \mathbf{s} each:

$$mCE = (\sum_{s=1}^5 \sum_{c=1}^{19} E_{s,c}) / (5 * 19) \quad (3)$$

We additionally report **mCE** without the 4 noise corruptions the metric includes, which we denote **mCE_{xN}** (mean Corruption Error ex Noise). This metric evaluates robustness against the remaining 15 corruption types that are not based on any form of pixel-wise noise, like the p -norm corruptions we train on. To cover random p -norm corruptions, we introduce a robustness metric **mCE_{L_p}** (mean Corruption Error p -norm), which is calculated in a similar way as (3) from the average of error rates. As shown in Table 1, the corruptions \mathbf{c} for **mCE_{L_p}** are 9 different p -norms and the severities \mathbf{s} are 10 different ϵ -values for each p -norm. The p -norms and ϵ -values were manually selected to cover a wide range of values and lead to significant and comparable performance degradation of a standard model.

In order to investigate imperceptible random p -norm corruptions, we propose the **iCE** (imperceptible Corruption Error) metric:

$$iCE = (\sum_{i=1}^n E_i - E_{clean}) / (n * E_{clean}), \quad (4)$$

where n is the number of different imperceptible corruptions. This metric can be considered as a minimum requirement for the corruption robustness of a classifier. **iCE** quantifies the increase in error rate relative to the clean error rate E_{clean} and is therefore reported in %. For every dataset in our study, we chose $n = 6$ p -norm corruptions (Table 1). We select p and ϵ -values based on a small batch of randomly sampled and maximally corrupted images. Figure 2 visualizes such corruptions compared to the original image for the CIFAR and TinyImageNet datasets.

Table 1: Sets of p -norm corruptions for calculating the mCE_{L_p} and **iCE** metrics. Brackets contain the minimum and maximum out of 10 ϵ -values for each p -norm. For L_0 , ϵ is the ratio of maximally corrupted image dimensions.

p	$mCE_{L_p} [\epsilon_{min}, \epsilon_{max}]$		$iCE [\epsilon]$	
	CIFAR	TIN	CIFAR	TIN
0	[0.005, 0.12]	[0.01, 0.3]		
0.5	[2.5e+4, 4e+5]	[2e+5, 1.2e+7]	2.5e+4	7e+5
1	[12.5, 200]	[37.5, 1500]	25	125
2	[0.25, 5]	[0.5, 20]	0.5	2
5	[0.03, 0.6]	[0.05, 1.5]		
10	[0.02, 0.3]	[0.02, 0.7]	0.03	0.06
50	[0.01, 0.18]	[0.02, 0.35]	0.02	0.04
200	[0.01, 0.15]	[0.02, 0.3]	0.01	0.01
∞	[0.005, 0.15]	[0.01, 0.3]		

4.2 Training Setup

Experiments are performed on the CIFAR-10 (C10), CIFAR-100 (C100) (Krizhevsky et al., 2009) and Tiny ImageNet (TIN) (Le and Yang, 2015) classification datasets. We train 3 architectures of convolutional neural networks: A WideResNet28-4 (WRN) with 0.3 dropout probability (Zagoruyko and Komodakis, 2016), a DenseNet201-12 (DN) (Huang et al., 2017) and a ResNeXt29-32x4d (RNX) (Xie et al., 2017) model. We use a Cosine Annealing Learning Rate schedule with 150 epochs and an initial learning rate of 0.1 that restarts after 10, 30 and 70 epochs (Loshchilov and Hutter, 2016). As an optimizer, we use SGD with 0.9 momentum and 0.0005 learning rate decay. We use a batch size of 384, resize the image data to the interval [0,1] and augment with random horizontal flips and random crops.

In addition to standard training, we apply a set of p -norm corruptions to the training dataset with different ϵ -values each. $L_0, L_{0.5}, L_1, L_2, L_{50}$ and L_∞ norms are used. $L_1(40)$ denotes a model trained exclusively on data augmented with L_1 corruptions with $\epsilon \leq 40$. We manually selected the set of p -norms to cover a wide range of values and the 2 ϵ -values for each p -norm so that we observe a meaningfully large effect on the metrics for all p -norms.

We also train on combinations of p -norm corruptions on one model by randomly applying one from a wider set of p -norm corruptions and ϵ -values. An overview of the 3 different combined corruption sets is shown in Table 2, denoted C1, C2 and C3. For all p -norm corruptions at training time, we apply the same corruption sample to a minibatch of 8 images to circumvent computational drawbacks.

Furthermore, the p -norm corruption combinations are compared and combined with the 4 state-of-the-art

Table 2: Sets of p -norm corruptions for the training of the models C1, C2 and C3. Brackets contain the minimum and maximum out of 10 (C1 and C2) or 5 (C3) ϵ -values for each p -norm.

p	$[\epsilon_{min}, \epsilon_{max}]$			
	C1	C2	C3 on CIFAR	C3 on TIN
0	+	+	[0.005, 0.03]*	[0.01, 0.075]*
0.5	+		[2.5e+4, 1.5e+5]*	[2e+5, 1.8e+6]*
1	+		[12.5, 75]*	[37.5, 300]*
2	+	+	[0.25, 1.5]*	[0.5, 4]*
5	+		[0.03, 0.2]*	[0.05, 0.3]*
10	+		[0.02, 0.1]*	[0.02, 0.14]*
50	+		[0.01, 0.06]*	[0.02, 0.1]*
200	+		[0.01, 0.05]*	[0.02, 0.08]*
∞	+	+	[0.005, 0.04]*	[0.01, 0.06]*

+ Same ϵ -values as in mCE_{L_p} for this p -norm (see Table 1
* Lowest 5 of the 10 ϵ -values in mCE_{L_p} for this p -norm
(see Table 1

data augmentation and mixing strategies TrivialAugment (TA) (Müller and Hutter, 2021), RandAugment (RA) (Cubuk et al., 2020) and AugMix (AM) (Hendrycks et al., 2019) and Mixup (MU) (Zhang et al., 2018). Accordingly, TA+C1 denotes a model trained on images with TA augmentation followed by the C1 corruption.

5 RESULTS

Table 3 compares different models trained with p -norm corruptions on the CIFAR-100 dataset with respect to the metrics described above. The table shows that all corruption-trained models produce improved mCE and mCE_{L_p} values at the expense of clean accuracy. Increasing the intensity of training corruptions mostly increases this effect. L_0 training is an exception where this effect is inconsistent. We find that there is much less positive effect of corruption training on mCE_{xN} . For corruption training outside of L_0 , increasing the intensity of corruptions actually degrades mCE_{xN} . The combined corruption models C1, C2 and C3 achieve much higher improvements in robustness than the models trained on one corruption only at a similar degradation of clean accuracy. In particular, they achieve significantly improved mCE_{xN} robustness. Model C2 performs better than C1 overall. C3 achieves slightly less robustness against noise (mCE and mCE_{L_p}), but better clean accuracy. The standard model and the models trained on L_0 corruptions reveal significant iCE values, while iCE is near zero for all other models.

Table 4 illustrates the effect of a selection of train-

Table 3: All metrics for the DenseNet model on CIFAR-100. We compare standard training data with various p -norm corrupted training data and combinations of p -norm corrupted training data.

Model	E_{clean}	mCE	mCE_{xN}	mCE_{L_p}	iCE
Standard	23.21	51.33	46.19	53.70	12.41%
$L_0(0.01)$	24.08	47.32	45.76	45.57	8.6%
$L_0(0.03)$	23.62	47.24	44.80	47.25	7.7%
$L_{0.5}(7.5e+4)$	25.86	47.91	45.83	41.22	-1.0%
$L_{0.5}(1.5e+5)$	26.35	43.11	44.15	33.83	-0.1%
$L_1(50)$	25.68	47.78	45.11	41.86	-1.0%
$L_1(100)$	29.12	45.64	46.28	34.12	-0.1%
$L_2(1)$	24.77	48.92	45.71	44.06	0.0%
$L_2(2.5)$	28.98	46.33	46.39	35.11	-0.4%
$L_{50}(0.03)$	24.82	48.67	45.27	44.87	-0.7%
$L_{50}(0.08)$	28.95	47.02	46.68	36.39	-0.5%
$L_{\infty}(0.02)$	25.05	48.63	45.47	43.79	-0.6%
$L_{\infty}(0.04)$	28.89	47.69	47.04	37.41	-0.2%
C1	27.51	39.66	41.85	29.67	0.8%
C2	26.04	39.31	41.75	28.38	0.9%
C3	24.60	40.30	41.73	29.88	0.7%

ing time p -norm corruptions and combined corruptions. To generalise the results, we report the delta of all metrics with the standard model, averaged over all model architectures. The table shows that L_0 corruption training slightly increases robustness, with the least negative impact on clean accuracy on the CIFAR datasets at the same time. The $L_{0.5}$ corruption training is the most effective among the single corruptions to increase mCE and mCE_{xN} . The L_{∞} corruption training is the least effective in terms of the ratio of robustness gained per clean accuracy lost. In fact, on the Tiny ImageNet dataset, no single p -norm corruption training significantly reduces mCE or mCE_{xN} . On all datasets, C1, C2 and C3 achieve the most significant robustness improvements. C3 stands out particularly on Tiny ImageNet, where it is the only model that improves clean accuracy while effectively reducing mCE or mCE_{xN} .

Figure 3 illustrates how the robustness obtained from training on different single p -norm corruptions transfers to robustness against other p -norm corruptions. It shows that L_0 corruptions are a special case. Training on L_0 corruptions gives the model very high robustness against L_0 corruptions, but less robustness against all other p -norm corruptions compared with other training strategies. At the same time, no p -norm corruption training except L_0 effectively achieves robustness against L_0 corruptions. Except for the L_0 -norm, robustness from training on all other p -norm corruptions transfers across the p -norms. However,

Table 4: The effect of p -norm corruption training types relative to standard training, averaged across all model architectures and averaged for the two CIFAR datasets.

Model	ΔE_{clean}	ΔmCE	ΔmCE_{xN}	ΔmCE_{L_p}
CIFAR				
$L_0(0.01)$	+0.3	-4.3	-0.72	-8.96
$L_{0.5}(7.5e+4)$	+1.14	-6.15	-1.73	-10.62
$L_2(1)$	+1.12	-3.69	-1.18	-11.89
$L_\infty(0.02)$	+1.51	-2.74	-0.33	-10.9
C1	+2.51	-13.04	-4.95	-27.42
C2	+1.79	-12.95	-4.78	-27.86
C3	+1.06	-10.8	-3.45	-25.82
TIN				
$L_0(0.02)$	+0.18	-0.8	+0.05	-4.06
$L_{0.5}(1.2e+6)$	-0.11	-0.22	+0.52	-4.39
$L_2(2)$	+0.02	+0.27	+0.82	-2.96
$L_\infty(0.04)$	+0.77	+0.95	+2.22	-4.47
C1	+1.46	-2.57	-0.46	-14.67
C2	+0.41	-2.81	-0.74	-15.52
C3	-0.14	-2.69	-0.79	-12.13

corruptions of lower p -norms such as $L_{0.5}$ and L_1 are more suitable for training than corruptions of higher norms such as L_{50} and L_∞ . The former actually achieves higher robustness against L_∞ -norm corruptions than L_∞ -norm training itself.

Table 5 illustrates the effectiveness of the data augmentation strategies RA, MU, AM and TA. RA and TA were not evaluated for corruption robustness in the original publications. the results show that all methods improve both clean accuracy and robustness. TA achieves the best E_{clean} values. It leads to high robustness values on the CIFAR datasets and especially on the WRN model. AM is the most effective method overall in terms of robustness. Our results show that MU, AM and TA can be improved by adding combined p -norm corruptions. For the CIFAR datasets, additional combined p -norm corruption training only leads to increases in mCE and mCE_{L_p} , but not mCE_{xN} . On Tiny Imagenet, such additional corruptions can, in some combinations, increase mCE_{xN} in addition to MU, AM and TA, without any loss of clean accuracy.

All data augmentation strategies still achieve a significant iCE value when not trained with additional corruptions. The iCE value is much lower for Tiny Imagenet than for CIFAR.

Figure 4 visualizes both E_{clean} and mCE for selected model pairs, where one of the pairs is additionally trained with C1 or C2. Models towards the lower left corner are both more accurate and more robust. The arrows illustrate how C1 and C2 training can mit-

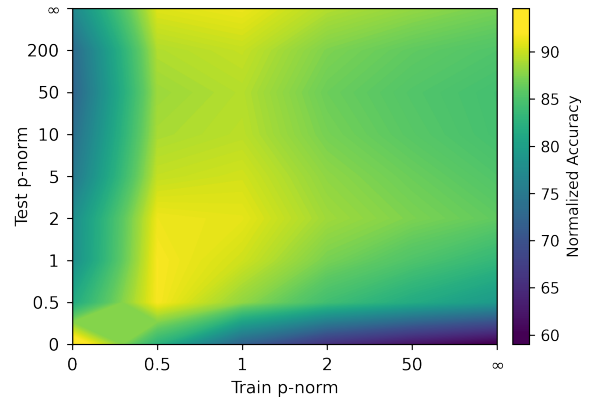


Figure 3: Normalized accuracy when training and testing on different p -norm corruptions. For each test corruption (see mCE_{L_p} in Table 1), the accuracies of all models trained on p -norm corruptions (without additional data augmentation strategies) are first normalized so that the best model achieves 100% accuracy. Then the average accuracy is calculated across all model architectures and datasets as well as across all ϵ -values of the same p -norm for training and testing. This visualizes how, on average, training on one p -norm leads to robustness against all p -norm corruptions. The prior normalization makes the trained models comparable.

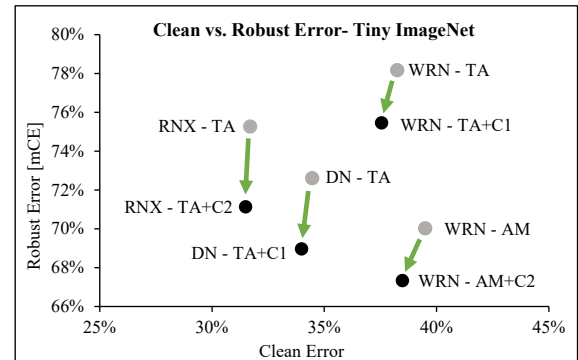


Figure 4: Clean Error vs. mCE plot for selected models on Tiny Imagenet. The green arrows indicate an improvement of both metrics when the model is trained on p -norm corruption combinations.

igate the trade-off between accuracy and robustness in these cases.

Figure 6 in the appendix shows how training data augmentation has an implicit regularizing effect on the training process, flattening the learning curve. This effect is evident for the C1 combination, although much less significant than for TA. Strong random training data augmentation can allow for a longer training process (Vryniotis, 2021).

Table 5: The performance of state-of-the-art data augmentation techniques with additional p -norm corruption combinations. For WRN and RNX, we show those data augmentations that are most effective for at least one metric. The full results are available on Github.

Model	E_{clean}	mCE	mCE_{xN}	mCE_{L_p}	iCE	E_{clean}	mCE	mCE_{xN}	mCE_{L_p}	iCE	E_{clean}	mCE	mCE_{xN}	mCE_{L_p}	iCE
	CIFAR-10				CIFAR-100				TinyImageNet						
DN															
Standard	5.37	25.38	20.72	28.16	17.2%	23.21	51.33	46.19	53.70	12.4%	37.38	76.46	75.28	53.82	1.4%
RA	4.59	18.25	14.91	21.76	19.0%	21.81	43.87	39.19	49.66	9.6%	35.84	74.53	73.81	52.49	1.4%
MU	4.64	23.39	17.65	29.17	14.7%	22.16	48.96	42.67	53.22	7.7%	35.13	72.81	71.49	50.43	0.6%
MU+C1	5.68	13.89	15.44	7.03	2.1%	23.92	36.96	39.39	26.21	0.5%	36.75	71.40	72.10	38.86	0.2%
MU+C2	5.36	13.77	15.28	6.98	3.5%	23.40	36.88	39.31	25.95	0.6%	35.87	70.79	71.35	38.05	0.5%
MU+C3	4.92	14.65	15.35	8.42	1.9%	22.84	38.22	39.50	28.17	0.2%	35.27	71.20	72.12	42.47	0.4%
AM	4.88	13.14	11.69	13.21	4.6%	23.27	37.90	35.85	37.11	3.6%	36.80	67.03	66.42	49.13	1.9%
AM+C1	5.94	11.32	12.15	7.14	1.1%	25.17	34.86	36.37	27.56	1.0%	38.15	65.19	65.65	40.13	0.2%
AM+C2	5.30	10.58	11.34	6.75	2.1%	24.98	34.50	35.96	27.40	1.2%	38.10	65.02	65.30	40.17	0.2%
AM+C3	5.08	11.34	11.48	8.15	3.6%	24.30	35.32	35.81	29.24	1.0%	37.08	64.12	65.12	43.20	0.5%
TA	4.43	14.25	11.12	17.08	8.4%	20.04	37.85	33.25	42.71	9.0%	34.46	72.61	72.39	72.36	0.7%
TA+C1	5.19	11.94	13.07	6.63	3.3%	22.74	35.27	37.34	25.52	1.2%	33.99	68.97	69.58	36.27	0.2%
TA+C2	5.01	12.88	14.21	6.68	2.3%	22.43	35.32	37.40	25.34	1.4%	34.40	69.91	70.43	36.90	0.5%
TA+C3	4.88	13.36	14.16	7.63	1.8%	21.92	36.36	37.82	26.61	0.5%	34.01	71.48	73.46	40.53	0.4%
WRN															
RA	4.56	21.80	18.45	24.02	12.1%	23.25	48.65	44.77	50.96	7.8%	36.89	75.2	73.99	54.05	3.0%
AM+C2	5.53	13.39	14.72	7.13	2.1%	25.40	37.08	39.03	28.01	0.6%	38.48	67.34	67.46	41.22	0.5%
TA	4.13	15.45	11.87	18.68	7.0%	21.70	41.87	37.81	44.32	8.2%	38.25	78.18	77.92	77.88	1.6%
RNX															
AM	4.35	14.06	12.13	14.94	9.2%	21.45	38.10	35.31	39.39	4.5%	34.97	67.79	66.09	47.85	1.7%
AM+C2	5.87	11.83	12.87	7.25	2.0%	24.22	33.95	35.60	26.59	0.8%	35.03	65.01	65.52	37.51	0.7%
TA	4.14	15.56	12.55	18.62	10.5%	19.55	37.80	34.28	40.44	6.6%	31.70	75.27	74.98	74.95	2.0%
TA+C2	5.27	14.09	15.86	6.72	0.7%	21.28	35.09	37.52	24.48	1.5%	31.49	71.13	71.99	34.20	0.9%

6 DISCUSSION

Vulnerability to Imperceptible Corruptions For the CIFAR datasets in particular, we found iCE values of well above 10%. Models trained with state-of-the-art data augmentation methods are still equally vulnerable to imperceptible random noise. Training with arbitrary noise outside L_0 corruptions solves the problem. We recommend that the set of imperceptible corruptions be further developed as a minimum requirement for the robustness of vision models, and that metrics such as iCE be evaluated for this purpose.

Robustness transfer to Real-World Corruptions From our experiments we derive insights into improving real-world robustness by training with p -norm corruptions:

- Training with single p -norm corruptions generally leads to mCE improvements only on CIFAR, not on Tiny ImageNet. The improvements are mainly attributable to the noise types within mCE . There

is little to negative transfer of robustness against corruption types outside the pixel-wise noise, represented by the mCE_{xN} metric.

- Training with combinations of p -norm corruptions leads to robustness improvements for the majority of corruption types outside of pixel-wise noise⁶. Thus, mCE_{xN} even improves on Tiny ImageNet.
- RA, MU, AM and TA show significant robustness improvements against all real-world corruptions.
- Adding p -norm corruption combinations to RA, MU, AM and TA gives mixed results. While mCE often improves, mCE_{xN} does so less often. For Tiny ImageNet, C2 improves mCE_{xN} quite effectively on top of all other data augmentation strategies. For CIFAR, mCE_{xN} could not be improved significantly beyond AM and TA.

⁶Visit Github for all individual results

Robustness transfer across p -norms Given the limited transferability of robustness between different types of corruptions known from the literature and the differences in volume for different p -norm balls (Table 6), we expected models trained on one p -norm to achieve high robustness against that p -norm in particular. However, we found that training on p -norm corruptions outside of L_0 leads to good robustness against all p -norm corruptions outside of L_0 . We find that training on L_∞ -norm corruptions performs worse overall compared to other p -norms. The L_0 corruption seems to be a special case that generalizes mainly to itself. We investigate this behaviour by examining whether p -norm corruptions overlap in the input space (see Figure 5 in the appendix).

We find that the random L_0 corruptions are a special case in that they almost never share the same input space with an L_2 -norm ball, and vice versa. In a slightly weaker form, this is also true when comparing L_∞ -norm and L_2 -norm corruptions. However, when comparing other p -norm corruptions with L_2 -norm corruptions, we find that for most ϵ values the corruptions overlap each other. The observations from Figure 5 explain, from a coverage perspective, why corruption robustness seems to transfer between different p -norms outside of L_0 . L_∞ -norm corruptions also appear to be a corner case in Figure 5, as they are largely distinct from L_2 -norm corruptions. This is in contrast to our empirical finding that robustness against L_∞ -norm corruptions is more effectively achieved by training on other p -norm corruptions.

From the Figures 3 and 5 we conclude that it makes little difference to train and test on a variety of random p -norm corruptions with $0 < p < \infty$. This is especially true when the ϵ -values are chosen arbitrarily, such as for the set of corruptions in the mCE_{L_p} -metric. Most corruptions from these norms will only be sampled in the same region of the input space and, therefore, train or test the same model property.

Promising Data Augmentation Strategies From our investigations of robustness transfer across p -norms we also conclude that the combined corruption training strategy C2 generally makes more sense than C1, since it contains only one p -norm corruption with $0 < p < \infty$. On average, we find evidence for this assumption in our data, where C2 achieves similar robustness gains at a lower cost of clean accuracy. In future work, we would like to investigate whether the C2 combination can be further improved. First, the ineffective L_∞ corruption could be reduced or eliminated. Second, L_2 could be replaced by the apparently more effective $L_{0.5}$ or L_1 -norm corruptions, or by simple Gaussian noise.

All data augmentation methods MU, RA, AM and

TA improve both corruption robustness and clean accuracy and are therefore highly recommended for all models and datasets. It is therefore important to see whether p -norm corruptions can be combined with these methods. Our experiments show a mixed picture: Robustness against noise can be improved, but robustness against corruptions outside of noise less often. The results vary across datasets, model architectures, and base data augmentation methods, as well as across the different severities of p -norm corruptions (C1 vs C3). Future progress on this topic requires precise calibration of the p -norm corruption combinations and possibly multiple runs of the same experiment to account for the inherent randomness of the process and to obtain representative results. In future work, we aim to improve the p -norm corruption combinations and apply them for more advanced training techniques as in (Lim et al., 2021). We believe that this study provides arguments in principle that corruption combinations are more effective than single noise injections.

7 CONCLUSION

Robustness training and evaluation with random p -norm corruptions has been little studied in the literature. We trained and tested three classification models with random p -norm corruptions on three image datasets. We discussed how robustness transfers across p -norms from an empirical and test coverage perspective. The results show that training data augmentation with L_0 -norm corruptions is a specific corner case. Among all other p -norm corruptions, lower p are more effective for training models. Combinations of p -norm corruptions are most effective, which can achieve robustness against corruptions other than pixel-wise noise. Depending on the setup, p -norm corruption combinations can improve robustness when applied in sequence with state-of-the-art data augmentation strategies. We investigated three different p -norm corruption combinations and, based on our findings, made suggestions for further improving robustness. Our experiments show that several models, including those trained with state-of-the-art data augmentation techniques, are negatively affected by quasi-imperceptible random corruptions. Therefore, we emphasized the need to evaluate the robustness against such imperceptible corruptions and proposed an appropriate error metric for this purpose. In the future, we plan to further improve robustness by more advanced training data augmentation with corruption combinations.

REFERENCES

Calafiori, G., Dabbene, F., and Tempo, R. (1998). Uniform sample generation in l/\sub{p} balls for probabilistic robustness analysis. In *Proceedings of the 37th IEEE Conference on Decision and Control (Cat. No. 98CH36171)*, volume 3, pages 3335–3340. IEEE.

Carlini, N., Athalye, A., Papernot, N., Brendel, W., Rauber, J., Tsipras, D., Goodfellow, I., Madry, A., and Kurakin, A. (2019). On evaluating adversarial robustness. *arXiv preprint arXiv:1902.06705*.

Carlini, N. and Wagner, D. (2017). Towards evaluating the robustness of neural networks. In *2017 IEEE Symposium on Security and Privacy (SP)*, pages 39–57. IEEE.

Cohen, J. M., Rosenfeld, E., and Kolter, J. Z. (08.02.2019). Certified adversarial robustness via randomized smoothing. *International Conference on Machine Learning (ICML) 2019*, page 36.

Croce, F. and Hein, M. (2020). Reliable evaluation of adversarial robustness with an ensemble of diverse parameter-free attacks. In *International conference on machine learning*, pages 2206–2216. PMLR.

Cubuk, E. D., Zoph, B., Shlens, J., and Le, Q. V. (2020). Randaugment: Practical automated data augmentation with a reduced search space. In *Proceedings of the IEEE/CVF conference on computer vision and pattern recognition workshops*, pages 702–703.

Dai, W. and Berleant, D. (2021). Benchmarking robustness of deep learning classifiers using two-factor perturbation. In *2021 IEEE International Conference on Big Data (Big Data)*, pages 5085–5094. IEEE.

Dodge, S. and Karam, L. (2017). A study and comparison of human and deep learning recognition performance under visual distortions. In *2017 26th international conference on computer communication and networks (ICCCN)*, pages 1–7. IEEE.

Drenkow, N., Sani, N., Shpitser, I., and Unberath, M. (2021). A systematic review of robustness in deep learning for computer vision: Mind the gap? *arXiv preprint arXiv:2112.00639*.

Fawzi, A., Fawzi, H., and Fawzi, O. (2018a). Adversarial vulnerability for any classifier. *32nd Conference on Neural Information Processing Systems (NeurIPS 2018), Montréal, Canada*.

Fawzi, A., Fawzi, O., and Frossard, P. (2018b). Analysis of classifiers' robustness to adversarial perturbations. *Machine Learning*, 107(3):481–508.

Ford, N., Gilmer, J., Carlini, N., and Cubuk, E. D. (2019). Adversarial examples are a natural consequence of test error in noise. *Prroceedings of the 36 th International Conference on Machine Learning (ICML), Long Beach, California, PMLR 97, 2019*.

Hendrycks, D. and Dietterich, T. (28.03.2019). Benchmarking neural network robustness to common corruptions and perturbations. *International Conference on Learning Representations (ICLR) 2019*, page 16.

Hendrycks, D., Mu, N., Cubuk, E. D., Zoph, B., Gilmer, J., and Lakshminarayanan, B. (05.12.2019). Augmix: A simple data processing method to improve robustness and uncertainty. *International Conference on Learning Representations (ICLR) 2020*, page 15.

Huang, G., Liu, Z., Van Der Maaten, L., and Weinberger, K. Q. (2017). Densely connected convolutional networks. In *Proceedings of the IEEE conference on computer vision and pattern recognition*, pages 4700–4708.

Huang, X., Kroening, D., Ruan, W., Sharp, J., Sun, Y., Thamo, E., Wu, M., and Yi, X. (2020). A survey of safety and trustworthiness of deep neural networks: Verification, testing, adversarial attack and defense, and interpretability. *Computer Science Review*, 37:100270.

Krizhevsky, A., Hinton, G., et al. (2009). Learning multiple layers of features from tiny images. *Toronto, Canada*.

Krizhevsky, A., Sutskever, I., and Hinton, G. E. (2017). Imagenet classification with deep convolutional neural networks. *Communications of the ACM*, 60(6):84–90.

Le, Y. and Yang, X. (2015). Tiny imagenet visual recognition challenge. *CS 231N, 2015*.

Lecuyer, M., Atlidakis, V., Geambasu, R., Hsu, D., and Jana, S. (2019). Certified robustness to adversarial examples with differential privacy. In *2019 IEEE symposium on security and privacy (SP)*, pages 656–672. IEEE.

Lim, S. H., Erichson, N. B., Utrera, F., Xu, W., and Mahoney, M. W. (2021). Noisy feature mixup. In *International Conference on Learning Representations*.

Lopes, R. G., Yin, D., Poole, B., Gilmer, J., and Cubuk, E. D. (2019). Improving robustness without sacrificing accuracy with patch gaussian augmentation. *arXiv preprint arXiv:1906.02611*.

Loshchilov, I. and Hutter, F. (2016). Sgdr: Stochastic gradient descent with warm restarts. In *International Conference on Learning Representations*.

Madry, A., Makelov, A., Schmidt, L., Tsipras, D., and Vladu, A. (19.06.2017). Towards deep learning models resistant to adversarial attacks. *International Conference on Learning Representations (ICLR) 2018*, page 28.

Mintun, E., Kirillov, A., and Xie, S. (2021). On interaction between augmentations and corruptions in natural corruption robustness. *Advances in Neural Information Processing Systems*, 34:3571–3583.

Müller, S. G. and Hutter, F. (2021). Trivialaugment: Tuning-free yet state-of-the-art data augmentation. In *Proceedings of the IEEE/CVF international conference on computer vision*, pages 774–782.

Rusak, E., Schott, L., Zimmermann, R. S., Bitterwolf, J., Bringmann, O., Bethge, M., and Brendel, W. (2020). A simple way to make neural networks robust against diverse image corruptions. In *European Conference on Computer Vision (ECCV)*, pages 53–69. Springer.

Shorten, C. and Khoshgoftaar, T. M. (2019). A survey on image data augmentation for deep learning. *Journal of big data*, 6(1):1–48.

Siedel, G., Vock, S., Morozov, A., and Voß, S. (2022). Utilizing class separation distance for the evaluation of corruption robustness of machine learning classifiers. *The IJCAI-ECAI-22 Workshop on Artificial In-*

telligence Safety (AISafety 2022), July 24-25, 2022, Vienna, Austria.

Szegedy, C., Zaremba, W., Sutskever, I., Bruna, J., Erhan, D., Goodfellow, I., and Fergus, R. (2013). Intriguing properties of neural networks. *arXiv preprint arXiv:1312.6199*.

Tsipras, D., Santurkar, S., Engstrom, L., Turner, A., and Madry, A. (2019). Robustness may be at odds with accuracy. In *International Conference on Learning Representations*.

Vryniotis, V. (2021). How to train state-of-the-art models using torchvision’s latest primitives. <https://pytorch.org/blog/how-to-train-state-of-the-art-models-using-torchvision-latest-primitives/>, 17.10.2023.

Wang, B., Webb, S., and Rainforth, T. (2021). Statistically robust neural network classification. In *Uncertainty in Artificial Intelligence*, pages 1735–1745. PMLR.

Wang, Z., Bovik, A., Sheikh, H., and Simoncelli, E. (2004). Image quality assessment: from error visibility to structural similarity. *IEEE Transactions on Image Processing*, 13(4):600–612.

Weng, T.-W., Chen, P.-Y., Nguyen, L. M., Squillante, M. S., Boopathy, A., Oseledets, I., and Daniel, L. (2019). Proven: Verifying robustness of neural networks with a probabilistic approach. *Proceedings of the 36th International Conference on Machine Learning, Long Beach, California, PMLR 97, 2019*.

Weng, T.-W., Zhang, H., Chen, P.-Y., Yi, J., Su, D., Gao, Y., Hsieh, C.-J., and Daniel, L. (2018). Evaluating the robustness of neural networks: An extreme value theory approach. *Sixth International Conference on Learning Representations (ICLR)*, page 18.

Xie, S., Girshick, R., Dollár, P., Tu, Z., and He, K. (2017). Aggregated residual transformations for deep neural networks. In *Proceedings of the IEEE conference on computer vision and pattern recognition*, pages 1492–1500.

Yang, Y.-Y., Rashtchian, C., Zhang, H., Salakhutdinov, R., and Chaudhuri, K. (2020). A closer look at accuracy vs. robustness. *34th Conference on Neural Information Processing Systems (NeurIPS 2020), Vancouver, Canada*.

Yun, S., Han, D., Oh, S. J., Chun, S., Choe, J., and Yoo, Y. (2019). Cutmix: Regularization strategy to train strong classifiers with localizable features. In *Proceedings of the IEEE/CVF international conference on computer vision*, pages 6023–6032.

Zagoruyko, S. and Komodakis, N. (2016). Wide residual networks. In *British Machine Vision Conference 2016*. British Machine Vision Association.

Zhang, H., Cisse, M., Dauphin, Y. N., and Lopez-Paz, D. (2018). mixup: Beyond empirical risk minimization. In *International Conference on Learning Representations*.

Zhang, H., Yu, Y., Jiao, J., Xing, E., El Ghaoui, L., and Jordan, M. (2019). Theoretically principled trade-off between robustness and accuracy. In *International conference on machine learning*, pages 7472–7482. PMLR.

APPENDIX

Volume of p -norm balls

Table 6: Volume factors between L_∞ -norm ball and L_2 -norm ball as well as L_2 -norm ball and L_1 -norm ball of the same ϵ in d -dimensional space

d	$p = [\infty, 2]$	$p = [2, 1]$
3	1.9	3.1
5	19.7	6.1
10	9037	401.5
20	$6 * 10^{10}$	$4 * 10^7$

Sampling Algorithm

We use the following sampling algorithm for norms $0 < p < \infty$, which returns a corrupted image I_c with maximum distance ϵ for a given clean image I of any dimension d :

1. Generate d independent random scalars $x_i = (G(1/p, 1))^{1/p}$, where $G(1/p, 1)$ is a Gamma-distribution with shape parameter $1/p$ and scale parameter 1.
2. Generate I -shaped vector x with components $x_i * s_i$, where s_i are random signs.
3. Generate scalar $r = w^{1/d}$ with w being a random scalar drawn from a uniform distribution of interval $[0, 1]$.
4. Generate $n = (\sum_{i=1}^d |x_i|^p)^{1/p}$ to norm the ball.
5. Return $I_c = I + (\epsilon * r * x/n)$

The factors r and w allow to adjust the density of the data points radially within the norm ball. We generally use a uniform distribution for w except when we sample imperceptible corruptions (Figure 2).

Volume overlap of high-dimensional p -norm balls

Figure 5 estimates the overlap of the volumes of two different p -norm balls with certain size ϵ and of dimensionality equal to CIFAR-10 (3072). We estimate their volumes by uniformly drawing 1000 samples from inside the norm ball. The figure shows 6 subplots for 6 different p -norms, with their respective ϵ being varied along the x-axis. The blue plots indicate how many samples from this first p -norm ball are also part of a second L_2 -norm ball with $\epsilon = 4$. Similarly, the orange plots show how many samples from the

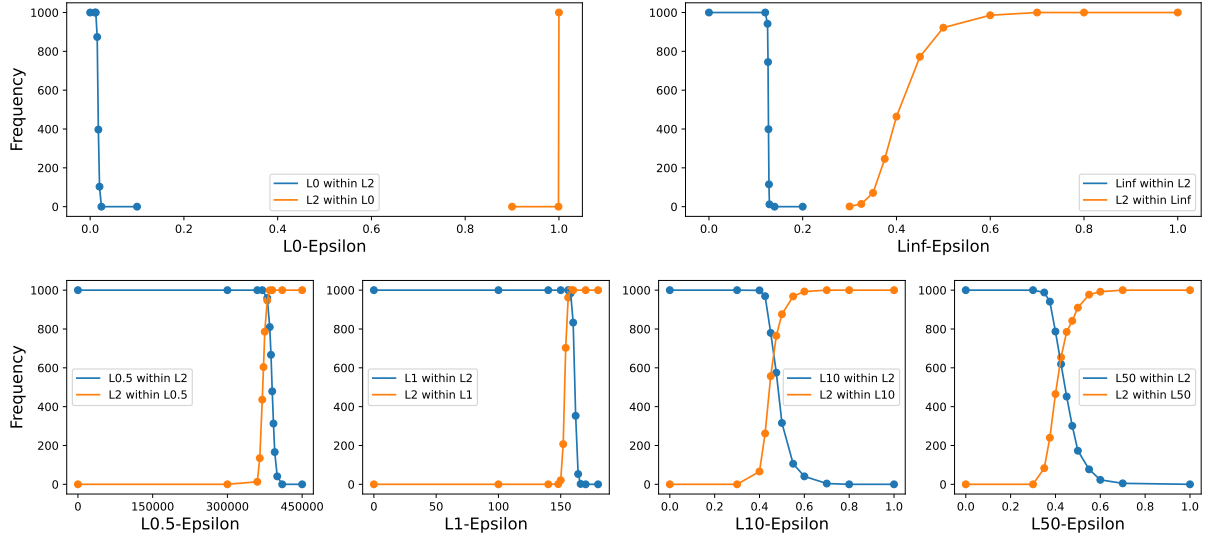


Figure 5: The frequency of 1000 samples drawn from inside a first CIFAR-10-dimensional p -norm ball also being part of a second L_2 -norm ball of $\epsilon = 4$ (blue plot), as well as the frequency of 1000 samples drawn from inside the second norm ball also being part of the first norm ball (orange plot).

second L_2 -norm ball are also part of the first norm ball.

There is a large interval of $L_0 - \epsilon$ -values, where the samples do not overlap. In a slightly weaker form, this also holds for random L_∞ -norm corruptions. This implies that when comparing L_2 -norms with L_0 -norms or L_∞ -norms, there is a large range of ϵ -values, where the two norm balls cover predominantly different regions of the input space. However, when comparing other p -norms besides of L_0 and L_∞ with L_2 , as has been done in the second row of Figure 5, a different result can be observed. One of the norm balls predominantly overlaps the other in volume for the major range of ϵ -values.

Learning Curve Effect

When added to a standard or TA training procedure, the training curve of the C1 model is more flat (Figure 6). TA itself shows a very strong flattening effect on the learning curve and requires visibly more epochs to converge.

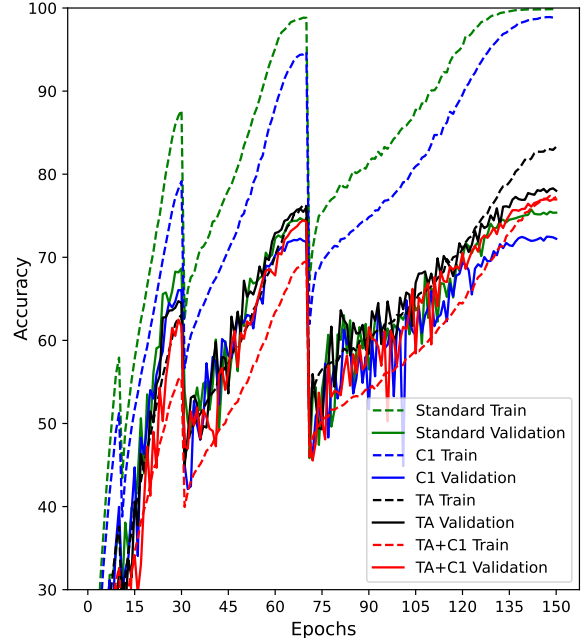


Figure 6: Training and validation learning curves of various models show the slight regularizing effect of p -norm corruptions in the C1 combination on the training process.